



1 **Ensemble Projection of the Sea Level Rise Impact on Storm Surge** 2 **and Inundation in the Coastal Bangladesh**

3 Mansur Ali Jisan¹, Shaowu Bao¹, Leonard J. Pietrafesa¹

4 ¹Department of Coastal and Marine Systems Science, Coastal Carolina University, Conway, South Carolina, United States.

5 *Correspondence to:* Mansur Ali Jisan (mjisan@g.coastal.edu)

6 **Abstract.**

7 The hydrodynamic model Delft3D is used to study the impact of Sea Level Rise (SLR) on storm surge and inundation in the
8 coastal region of Bangladesh. To study the present day inundation scenario, track of two known tropical cyclones (TC) were
9 used: Aila (Category 1; 2009) and Sidr (Category 5; 2007). Model results were validated with the available observations. Future
10 inundation scenarios were generated by using the strength of TC Sidr, TC Aila and an ensemble of historical TC tracks but
11 incorporating the effect of SLR.

12 Since future change in storm surge inundation under SLR impact is a probabilistic incident, that's why a probable range of future
13 change in inundated area was calculated by taking in to consideration the uncertainties associated with TC tracks, intensities and
14 landfall timing.

15 The model outputs showed that, the inundated area for TC Sidr, which was calculated as 1860 km², would become 31% higher
16 than the present day scenario if a SLR of 0.26 meter occurs during the mid-21st century climate scenario. Similar to that, an
17 increasing trend was found for the end of the 21st century climate scenario. It was found that with a SLR of 0.54 meter, the
18 inundated area would become 53% higher than the present day case.

19 Along with the inundation area, the impact of SLR was examined for the changes in future storm surge level. A significant
20 increase of 21% was found in storm surge level for the case of TC Sidr in Barisal station if a Sea Level Rise of 0.26 meter occurs
21 at the middle of the 21st century. Similar to that, an increase of 37% was found in storm surge level with a SLR of 0.54 meter in
22 this location for the end of the 21st century climate scenario.

23 Ensemble projections based on uncertainties of future TC events also showed that, for a change of 0.54 meters in SLR, the
24 inundated area would range between 3500-3750 km² whereas for present day SLR simulations it was found within the range of
25 1000-1250 km²

26 These results revealed that even if the future TCs remain at the same strength as at present, the projected changes in SLR will
27 generate more severe threats in terms of surge height and extent of inundated area.

28

29

30

31

32



33 1. Introduction

34

35 In addition to routine inundation from upstream river water and the downstream tides, the coastal part of Bangladesh is
36 frequently flooded by storm surges induced by tropical cyclones (TCs). Typically, TC-induced storm surges in this area initiate
37 in the central or southern part of the Bay of Bengal or near the Andaman Sea. TCs normally occur during April – May, the pre-
38 monsoon period, and again from October – November, the post monsoon period. Harris (1963) mentioned that five basic
39 processes (i.e., pressure, direct wind, earth's rotation, waves and rainfall effects) cause water level rise under storm conditions.
40 Pietrafesa *et al.* (1986) also pointed out that high water at the mouths of coastal estuaries, bays and rivers can block discharges of
41 upstream waters and contribute to upstream flooding; a non-local effect. Among these processes, storm surges form primarily
42 due to the TC wind stresses mechanically driving the surface frictional layer onshore. Assuming an idealized balance between
43 pressure gradient force and surface wind stress with assumed small bottom stress, the surge related to TC wind stress can be
44 expressed as $\Delta h = \frac{\tau_w L}{g\rho h}$, where L is the fetch of the wind (the distance over which the wind blows), τ_w is the wind stress due to the
45 friction between the moving air and water surface, g is the gravity, ρ is the density of water, h is the depth near the coast (Hearn,
46 2008). Also, as a secondary process, due to the differences in pressure level, the water level rises in the areas of low atmospheric
47 pressure and falls in the areas of high atmospheric pressure, which is how the rising water level offsets the low atmospheric
48 pressure to keep the total pressure constant (Harris *et al.*, 1963).

49 According to Murty *et al.* (1986), the surge amplifies as it approaches the coast due to the shallow continental shelf of the Bay of
50 Bengal and hence it causes massive flooding in the low-lying coastal areas. A large percentage of the Bangladesh population
51 resides in the low lying coastal regions of the country. Most of the areas near the coastal zone of Bangladesh have been formed
52 by the process of riverine sedimentation and because of that the low lying areas are relatively flat and as such are susceptible to
53 flooding even under normal astronomical tide conditions. Furthermore, the triangular shape of the Bay of Bengal region makes
54 storm surges more distressing, as a funneling effect occurs. The geomorphological characteristics of the region have made the
55 locale prone to major TC events, events which have occurred multiple times in the past, directly causing the deaths of hundreds
56 of thousands of lives (Haque, 1997). This type of coastal flooding associated with the changes in coastal water level due to
57 storms passing over the sea causes great loss of human lives, property, livelihoods and the economy of the country (Haque,
58 1997).

59 Future climate change scenarios may further exacerbate the threats of TC-induced storm surge and inundation. According to the
60 Intergovernmental Panel on Climate Change Fourth Assessment Report (IPCC 4AR), there is a high probability of major
61 changes in TC activity across various ocean basins including the Arabian Sea and the Bay of Bengal. According to Milliman *et al.*
62 (1989), this Ganges-Brahmaputra-Meghna Delta region has long been characterized as a highly vulnerable zone due to its
63 exposure to the increasing trend of SLR. According to the SLR analysis done by the South Asian Association for Regional
64 Cooperation based on the 22-year records of observed sea level at Charchanga, Cox's Bazar and Hiron Point, sea level is rising
65 at rates of 6.0, 7.8 and 4 mm/year, respectively in those three locations (SMRC, 2003). These rates are much higher than the
66 global rate of SLR (~ 3.2 mm/year) over the last 25 years (Pietrafesa *et al.*, 2016). Based on Warrick *et al.* (1996), the sea level in
67 the Bay of Bengal is also influenced by local factors including tectonic setting, deltaic processes and sediment load; for example,
68 the coastal region of Bangladesh has been subsiding due to the pressure on the Earth's crust from the sediment with thick layers
69 that has formed over millions of years. Warrick *et al.* (1996) also analyzed the recent history of land accretion and suggested that
70 the subsidence is also balanced by land accretion due to sediment supply from the coast. These physical phenomena have been



71 shaping the coast of Bangladesh over the past 100 years. A global SLR of 26-59 cm has been projected over the next 84 years to
72 2100 by the IPCC under the scenario A1F1 (Meehl et al. 2007). In this proposed work, we will use the SLR projections from
73 Caesar et al. (2017; under review), which suggests a projection of SLR of 26 cm for the mid-21st century (2040 -2060) and 54
74 cm for the end-21st century (2079 -2099).

75 Previous studies have analyzed the likely impact of climate change, especially SLR, on storm surge and inundation in this region.
76 Using hydrodynamic models, Ali (1992) showed that with an increase of 1.0 and 1.5 meters of SLR, 10% and 15.5%,
77 respectively, of the entirety of Bangladesh would get flooded under the strength of future TCs. Karim and Mimura (2008) used a
78 1-D hydrodynamic model to study the inundation under several scenarios of climate and for the case of future TCs by changing
79 sea surface temperature, SLR, wind speed and sea level pressure. Based on their results, Karim and Mimura (2008) concluded
80 that with an increase of 2°C in SST and 0.3 meters of SLR, the flood risk area would be 15.3% more than the present day risk
81 area and the depth of flooding would increase by as much as 22.7% within 20 km from the coastline. Both Ali (1992) and Karim
82 & Mimura (2008) considered SST rise and future strength of TCs in simulating the future storm surge and inundation.

83 However, the impact of climate change on the frequency and intensity of TCs are still debatable (Knutson *et al.*, 2010). The
84 projection of the TC characteristics in the Bay of Bengal region is unclear as well. To improve these uncertainties, a reasonable
85 method to examine the impact of future SLR on storm surge and inundation would be to construct an ensemble of tracks and
86 intensities of possible land-falling TCs along the Bangladesh coast based on the historical TC records. From this statistical
87 approach, we can quantify the probable impact of TC tracks under future SLR change. To date, such an approach has not been
88 done and will be method of this study.

89 We first use Delft3D to simulate the present day storm surge and inundation using the strength of two recent TCs (TC Sidr and
90 TC Aila), and validate the simulations with observational data. Future storm surge and inundation scenarios were then generated
91 by incorporating the projected SLR.

92 The study was carried out in the Ganges-Brahmaputra-Meghna Delta regions (Figure 1). According to Integrated Coastal Zone
93 Management Plan, 19 districts of Bangladesh located near the Bay of Bengal area were defined as the coastal areas. We've
94 considered all those in this study. We selected two TC cases in this study, a strong Saffir-Simpson(SS) Category-5 that directly
95 hit the study area, TC Sidr, and the other a SS Category -1 storm that made landfall in the South-West part of the study domain,
96 TC Aila.

97 TC Sidr made landfall near Barguna district (Figure 1) in 2007, causing ~ 3000 human fatalities and leaving millions homeless.
98 This category-5 cyclone is considered one of the most powerful cyclones in the past 15 years to have made landfall in
99 Bangladesh, which affected over nine millions people living across the Bangladesh coastal areas. The districts of Patuakhali,
100 Khulna, Barguna and Jhalokathi were badly affected. During TC Sidr, around 15% of the affected people took refuge in nearby
101 cyclone shelters. In the village of Angul Kata in Barguna district, around 1500 people took shelter in eight reinforced pillars to
102 protect themselves from the tidal surge of around 5 meters. If there had been no shelters, the death toll could have reached into
103 the hundreds in that area.

104 The other cyclone studied in this paper, TC Aila (Figure 1) occurred in the Bay of Bengal region in 2009. Although a category-1
105 storm, Aila caused ~ 190 deaths and affected 4.8 million people, the devastation that left a long term impact. The locales mainly
106 affected were Khulna, Patuakhali and Chandpur. The storm surge due to Aila broke a dam in Pataukhali and submerged five
107 villages, destroying a huge number of homes and leaving thousands of people homeless. Most of the people living in those



108 affected areas took shelter in the nearest cyclone shelters. According to government sources, approximately 2,500,000 houses
 109 had been destroyed completely and 3,700,000 houses had been damaged.

110 TC Sidr made landfall near Barguna district (Figure 1) in 2007, causing ~ 3000 human fatalities and leaving millions homeless.
 111 TC Aila occurred in the Bay of Bengal region in the year 2009 (Figure 1). Although a category-1 storm, Aila caused ~ 190
 112 deaths and affected 4.8 million people, devastation that left a long term impact. The locales mainly affected were Khulna,
 113 Patukhali and Chandpur. The storm surge due to Aila broke a dam in Pataukhali and submerged five villages, destroying huge
 114 number of homes and leaving thousands of people homeless.

115 2. Methodology

116 2.1 Modeling Methodology

117 2.1.1 Application of Numerical Model

118

119 For the purpose of developing present day and future inundation scenario in the coastal regions of Bangladesh, the Delft3D-
 120 FLOW (Delft Hydraulics, 2006), a multidimensional (2D or 3D) hydrodynamic and transport simulation program that calculates
 121 non-steady flow and transport phenomena resulting from tidal and meteorological forcing was used. Delft3D-FLOW solves the
 122 unsteady shallow water equation in two dimensions (depth-averaged) or in three dimensions. The system of equations consists of
 123 the horizontal equations of motion, the continuity equation, and the transport equations for conservative constituents. The
 124 equations are formulated in orthogonal curvilinear co-ordinates or in spherical co-ordinates. Delft3D – FLOW module’s two-
 125 dimensional, depth averaged flow equations can be applied for modeling tidal waves, storm surges, tsunamis, harbor oscillations
 126 (seiches) and transport of pollutants in vertically well-mixed flow regimes. In this paper Delft3D’s 2D mode for barotropic
 127 depth-integrated flow has been applied. The equations are listed below.

$$128 \quad \frac{\partial \zeta}{\partial t} + \frac{1}{\sqrt{G_{\xi\xi}\sqrt{G_{\eta\eta}}}} \frac{\partial[(d+\zeta)v\sqrt{G_{\eta\eta}}]}{\partial \xi} + \frac{1}{\sqrt{G_{\xi\xi}\sqrt{G_{\eta\eta}}}} \frac{\partial[(d+\zeta)v\sqrt{G_{\xi\xi}}]}{\partial \xi} = Q \quad (1)$$

$$129 \quad \frac{\partial u}{\partial t} + \frac{u}{\sqrt{G_{\xi\xi}}} \frac{\partial u}{\partial \xi} + \frac{v}{\sqrt{G_{\eta\eta}}} \frac{\partial u}{\partial \eta} + \frac{uv}{\sqrt{G_{\xi\xi}\sqrt{G_{\eta\eta}}}} \frac{\partial \sqrt{G_{\xi\xi}}}{\partial \eta} - \frac{v^2}{\sqrt{G_{\xi\xi}\sqrt{G_{\eta\eta}}}} \frac{\partial \sqrt{G_{\eta\eta}}}{\partial \xi} - f v + \frac{g}{\sqrt{G_{\xi\xi}}} \frac{\partial \zeta}{\partial \xi} = -\frac{1}{P_0 \sqrt{G_{\xi\xi}}} \frac{\partial P_{atm}}{\partial \xi} + F_{\xi} \quad (2)$$

$$130 \quad \frac{\partial v}{\partial t} + \frac{u}{\sqrt{G_{\xi\xi}}} \frac{\partial v}{\partial \xi} + \frac{v}{\sqrt{G_{\eta\eta}}} \frac{\partial v}{\partial \eta} + \frac{uv}{\sqrt{G_{\xi\xi}\sqrt{G_{\eta\eta}}}} \frac{\partial \sqrt{G_{\xi\xi}}}{\partial \eta} - \frac{u^2}{\sqrt{G_{\xi\xi}\sqrt{G_{\eta\eta}}}} \frac{\partial \sqrt{G_{\xi\xi}}}{\partial \eta} + f u + \frac{g}{\sqrt{G_{\xi\xi}}} \frac{\partial \zeta}{\partial \xi} = -\frac{1}{P_0 \sqrt{G_{\eta\eta}}} \frac{\partial P_{atm}}{\partial \eta} + F_{\eta} \quad (3)$$

131

132 where ξ , η are the spatial co-ordinates, ζ is representing water level above some horizontal plane of reference (m), u & v are the
 133 velocities in the ξ and η direction (m/s), d is the water depth below some horizontal plane of reference (m), g is the acceleration
 134 of gravity (m/s^2), P_{atm} is the atmospheric pressure at water surface ($kg/m/s^2$), Q is the discharge of water, evaporation or
 135 precipitation per unit area (m/s) , $\sqrt{G_{\xi\xi}}$ is the coefficient used to transfer one coordinate system into another one (m), F_{ξ} are the
 136 turbulent momentum flux in ξ -direction (m/s^2), F_{η} are the turbulent momentum flux in η -direction (m/s^2). Along with the
 137 appropriate set of initial and boundary conditions, the above-mentioned set of equations have been solved on an Arakawa-C type
 138 finite difference grid. Delft3D- FLOW manual (Delft Hydraulics, 2006) contains detailed information about these numerical
 139 aspects.



140 2.1.2 Model Grid and Bathymetry

141

142 The grid was set up using spherical coordinates, as displayed in Figure 1. The grid spacing varies from a minimum of 125
143 meters to a maximum of 1140 meters. The finer resolution was applied over land for calculating the inundation or wetting
144 process accurately. The bathymetries of the rivers and estuaries are specified using the cross sections measured by the Institute of
145 Water and Flood Management, Bangladesh. The land elevations are specified using the data from the Center for Environmental
146 and Geographic Information Services (CEGIS), Bangladesh. The ocean bathymetry is specified using the data from the General
147 Bathymetric Chart of the Oceans (BODC, 2003). Bathymetry and topographic data have been interpolated over the model
148 domain using triangular interpolation and grid-cell averaging methods.

149 2.1.3 Wind and Pressure Field

150

151 Track data of TCs Sidr and Aila were obtained from the Indian Meteorological Department (www.imd.gov.in). Using those data
152 as input, TC surface winds and mean sea level pressure fields were generated using the Wind Enhancement Scheme (WES)
153 (Heming et al. 1995) method based on the analytical equation by Holland (1980). Delft3D slightly improved the original WES
154 by introducing TC asymmetry. Unlike some previous method that incorporates TC wind asymmetry information from
155 observations (Xie et al. 2006), in WES the asymmetry was brought about by applying the translation speed of the cyclone center
156 displacement as steering current and by introducing rotation of wind speed due to friction (Heming et al. 1980).

157 According to the Holland's equation, gradient wind speed $V_g(r)$ at a distance r from the Centre of the cyclone is expressed as the
158 following:

$$159 V_g(r) = \left[\frac{AB(p_n - p_c) \exp\left(-\frac{A}{rB}\right)}{\rho r^B} + \frac{r^2 f^2}{4} \right]^{0.5} - rf/2 \quad (4)$$

160 Here ρ is the density of air, p_c is the central pressure and p_n is the ambient pressure, the Coriolis parameter is represented by f .
161 A and B are determined empirically; with the physical meaning of A as the relation of pressure or wind profile relative to the
162 origin, and parameter B defining the shape of the profile. Delft3D introduces a central pressure drop of $p_d = p_n - p_c$. By
163 equating $\frac{dV_g}{dr} = 0$, radius of maximum winds R_w can be given as follows:

$$164 R_w = A^{1/B} \quad (5)$$

165 Thus, R_w is independent of the relative values of ambient and central pressure and is defined entirely by the scaling parameters A
166 and B . Substitutions lead to the expression for the maximum wind speed V_m

$$167 V_m = \left[\frac{B p_d}{\rho e} \right]^{0.5} \quad (6)$$

168 Complete details about this method can be found in the user manual of Delft3D Flow (Delft Hydraulics, 2006).

169 The circular grid of TC wind fields used in this study consists of 36 columns and 500 rows and the data were updated at 6 hourly
170 intervals throughout its movement until the landfall. Figure 2 shows a snapshot of the wind field of TC Sidr over the model
171 domain, before landfall, generated using Holland's equation above.



172

173 **2.1.4 Roughness**

174 The spatially varying Manning's Roughness value has been defined based on land cover, such as vegetation, rivers and ocean
175 (Table 1). In the study domain, a mangrove forest, Sundarban, is located in the Southwest region, near TC Sidr's landfall
176 location (Figure 1). Sakib et al. (2015) found that Sundarban plays a significant role as a buffer in reducing the total inundation
177 during TC passages. Therefore, in this study, the mangrove region is considered.

178 In selecting the roughness values, methods described in Zhang et al. (2012) was followed and slightly modified values were
179 defined for the study area based on the vegetation types in that area.

180 **2.1.5 Boundary conditions**

181 Upstream boundaries were specified as discharges at the mouths of the three major rivers; the Ganges, the Brahmaputra & the
182 Upper Meghna; obtained from the Bangladesh Water Development Board (BWDB) as daily discharge. The downstream ocean
183 boundary was defined by the Topex/Poseidon Inverse Tidal model, based on Egbert et al. (1994) Location of the downstream
184 ocean boundary was shown in Figure 1

185 **2.2 Calculation Procedure for Present Day and Future Storm Surge and Inundation Scenario**

186

187 To generate storm surge and inundation for present day climate scenario, upstream discharge and downstream water level data
188 from the present day were used. For future SLR scenarios, present day hydrodynamic conditions and the strengths of present day
189 TCs were used but the future sea level was modified based on the SLR projections by Caesar et al. (2017; *under review*).
190 Scenarios were generated for both the Mid-21st century and the End-21st century time horizons for these TCs, Sidr and Aila.
191 Finally, comparisons were made in terms of storm surge and inundation to identify the changes between present day and future
192 SLR scenarios.

193 Now, future Storm surge inundation due to SLR is a probabilistic event that requires proper addressing of the uncertainties
194 associated with the input parameters. To address the future tropical cyclone uncertainties and obtain statistically significant
195 results, we created an ensemble of tropical cyclone tracks. The ensemble tracks were generated from different historical tropical
196 cyclones that made landfall over the study domain with different intensities. Along with the uncertainties associated with future
197 landfall locations, the intensity of Sidr-like and Aila-like TCs may be different. So, to address the uncertainty with the intensity,
198 we increased and decreased their intensity by 10% to simulate a probable range of future storm surge inundation.

199 Storm surge inundation can also be different based on landfall timing. If the storm would make landfall during the high tide
200 condition, flooding would be much higher at that time than what could happen during a low tide condition. We note that TC Sidr
201 and TC Aila made landfall during the high tide conditions, which may not always be applicable for the future TCs. To also
202 address uncertainties with the TC landfall timing, experiments were conducted by changing the timing of landfall to identify the
203 impact of high tide and low tide on storm surge and inundation. Here in this study, future storm surge inundation scenarios
204 caused by the ensemble tracks will then be simulated by incorporating the projected SLR. By taking all these parameters into
205 consideration, we conducted a total 108 ensemble simulations (36 for each; present day and two SLR scenarios). Parameters that
206 were considered in making ensemble projections shown in Table 2.



207 3. Results

208 3.1 Validation of the Model

209 Hourly tidal data from the Bangladesh Inland Water Transport Authority (BIWTA) was used to evaluate the performance of the
210 model used in this study. The model simulation's root mean square error (RMSE)⁷, mean absolute error (MAE)⁸ and dimension-
211 less Nash-Sutcliffe coefficient (E)⁹ (Nash and Sutcliffe, 1970) were calculated and listed in Table 3. A Nash-Sutcliffe coefficient
212 ranges between (-ve)infinity (no skill simulation) and one (perfect simulation).

213

$$214 \quad RMSE = \sqrt{\frac{\sum_{i=1}^n (X_{obs,i} - X_{model,i})^2}{n}} \quad (7)$$

$$215 \quad MAE = \frac{1}{n} \sum_{i=1}^n |X_{obs,i} - \hat{X}_{obs}| \quad (8)$$

$$216 \quad E = 1 - \frac{\sum_{i=1}^n (X_{obs,i} - X_{model,i})^2}{\sum_{i=1}^n (X_{obs,i} - \bar{X}_{obs})^2} \quad (9)$$

217

218 The simulated water levels were compared against the measured data from Bangladesh Inland Water Transport Authority
219 (BIWTA) at two locations: Barisal and Charchanga (Figure 1). Barisal station is located more towards the inland whereas
220 Charchanga is located near the coastline where the grid cell resolution was coarse. But none of them are in the open ocean water,
221 which is important to get a clear idea about storm surge level. TC Sidr made landfall near the Barisal Station (Figure 1) and the
222 impact of storm surge was clearer at the Barisal station than that of TC Aila, which made landfall outside the model domain
223 (Figure 1); therefore its impact was not as clear as that of Sidr.

224

225 In Figure 3(a) for TC Sidr at the Barisal station, the modeled water level, including storm surge and astronomical tides, was
226 slightly lower than the observations, and at the Charchanga station (Figure 3b) the measured water level variation displayed
227 larger amplitudes than did the model output, perhaps due to the coarse resolution of bathymetry. Similar types of variations
228 between measured and modeled water level was found for TC Aila (Figure 3c and Figure 3d). Nevertheless, the modeled water
229 level variations during TCs Sidr and Aila agreed reasonably well with measured data; as also confirmed by the average RMSE,
230 MAE and Nash-Sutcliffe coefficient. Therefore, we conclude that the method can be used to study the impact of SLR on storm
231 surge and inundation in future climate change scenarios.

232 3.2 Present Day Inundation Scenario

233

234 The storm surge inundation scenarios due to the two TCs considered were shown in Figure 4.

235 It can be seen from Figure 4 that the area flooded by TC Sidr (yellow shade+red shade) was much higher than the area flooded
236 by TC Aila (white shade+red shade), a result that is consistent with the fact that the category-5 TC Sidr was much stronger than
237 the category-1 TC Aila and directly hit the study area. The maximum sustained wind speed for TC Sidr was 260 km/h whereas
238 for TC Aila it was 110 km/h. The landfall location of Sidr was on the Eastern side of Sundarban, while for Aila, the landfall



239 location was towards the Western side of Sundarban. That explains why the inundations due to TC Sidr were located near the
240 eastern side of Sundarban, whereas for Aila, the inundation was located mainly in the western part. The extent of inundation due
241 to Sidr (1860 km²) was 35% larger than that of Aila (1208 km²)

242 Sakib et al. (2015) showed that Sundarban acted as a buffer zone in reducing the impact of Sidr and thereby reduced much of the
243 potential inundation depth and extent of flooding. As mentioned before, in the model simulation the impact of Sundarban was
244 realized using a higher Manning's roughness value as resistance for the surge to travel.

245 3.3 Impact of Future Climate Scenarios on Storm Surge Inundation

246

247 Future inundation scenarios were generated for two different time horizons: one for the mid-21st century and the other for the end
248 of the 21st century. The initial ocean water level was raised by 0.26 meters and 0.54 meters for the mid-21st century and end-21st
249 century, respectively. The upstream river discharge and downstream ocean water level were used from present day climate
250 scenarios.

251

252 In this section we seek to answer the question: if present day's TCs were to happen in future SLR scenarios, what storm surge
253 and inundation hazard would they cause? Therefore, the tracks and intensities of the two-present day TCs, Sidr and Aila, were
254 used as the model wind input parameters.

255

256 Figure 5 shows that under future SLR scenarios, the inundated areas would be significantly higher than those under the present-
257 day climate condition, as indicated by the white color shaded areas, for the TCs with the same strengths and landfall paths. For
258 the category-5 TC Sidr, the inundated area would be 31% and 53% higher than present day's 1860 km² inundated area, in mid-
259 21st century (0.26 meter SLR) and end of-21st century (0.54 meter SLR) climate scenarios, respectively (Figure 5a and Figure 5b)

260

261 Similarly, for TC Aila, a category 1 storm, there would be an increase in inundated areas. The calculated inundated area for TC
262 Aila under mid-21st century and end-of-21st century was found to be 1550 square kilometers and 1770 square kilometers
263 respectively (Figure 5c and Figure 5d) whereas for the present-day scenario it was found to be 1208 square kilometers.

264

265 All these simulations were done using present day tides, river discharges and the track and strength of present day TCs; while
266 changing the initial sea water level to reflect the effect of SLR. Therefore, the results suggest that even if the future TCs
267 strengths, the tides and river discharges remain the same as in the present, future SLR would significantly increase the inundated
268 area.

269 All of these simulations were done using present day tides, river discharges and the track and strength of present day TCs; while
270 changing the initial sea water level to reflect the effect of SLR. Therefore, the results suggest that even if the future TCs
271 strengths, the tides and river discharges remain the same as in the present, future SLR would significantly increase the inundated
272 area.

273 3.3.1 Ensemble Projection of Future Storm Surge Inundation

274 As discussed in section 2.2 that, future change in storm surge inundation can be different based on the intensity, landfall location
275 and timing of future TCs. By considering all those uncertainty factors mentioned in Table 2, a column plot was created (Figure



276 6) for present day sea level and future SLR scenarios. Ensemble simulation outputs also showed evidence for increase in the
277 inundated area under the effect of SLR. For the present day scenario (black column) out of 36 simulations, frequency of storm
278 surge inundation incidents that would likely occur between the range of 1000-1250 km² is 13 whereas for 0.26 meters of
279 SLR (red column), peak of the column shifted towards right side with a maximum frequency of inundation events occurred
280 within the range of 2000-2250 km² (10 times out of 36 simulation results). And for 0.54 meters of increase in sea level (blue
281 column), the peak of the column shifted more towards the right and the maximum number of simulation outputs (11 out of 36
282 simulations) showed the range of inundation to be within 3500-3750 km². These results show that even the change in intensities
283 of future TCs are indefinite and the landfall timing is uncertain, increase in sea level is going to increase the area of inundation.

284

285 **3.4 Impact of Sea Level Rise on Future Storm Surge Level**

286

287 In addition to the inundation area, SLR would also greatly affect storm surge levels. Similar to the approach used in the
288 inundation study (Section 3.3), TCs Sidr- and Aila-induced storm surges in the future SLR scenarios were simulated using their
289 recorded strengths.

290 The simulated storm surge water levels in future SLR scenarios were compared with both the observed and model generated
291 ones under the present day scenarios (Figure 7). It is to be mentioned that, while generating the future water level under the
292 effect of SLR, the baseline is only changing by considering the SLR effect and based on that factor the future storm surge level
293 was calculated. Other than that, the water level is the same as present day TCs.

294

295 From Figure 7 we can see that, for the case of TC Sidr the simulated storm surge level would become 2.3 meters (Figure 7a) in
296 Barisal station which is around 21% higher than the present day scenario. Similar to that, under the end-of-21st century 0.54
297 meters SLR scenario in Barisal, the storm surge would be around 37% higher (Figure 7a.) than the present day scenario and the
298 peak water level would reach 2.6 m.

299 Increase in storm surge was found at the Charchanga station also. For TC Sidr, under the mid-21st century scenario (0.26 meter
300 SLR), the model simulated storm surge level was found to be 14% higher (2.24 meters) (Figure 7b) than the present day and 31%
301 higher (2.59 m) (Figure 7b) than the present day for the end-of-21st century (0.54 m SLR) climate scenario.

302 For TC Aila in Barisal, the Storm Surge would become 22% higher than the present day, which was 1.61 meters under the 0.26
303 meters SLR condition for the mid-21st century climate scenario (Figure 7c). During the end-of-21st century climate scenario, the
304 increment would become even higher as the SLR would be 0.54 meter. Storm Surge would be 51% higher (1.96 meters) (Figure
305 7c) than the present day under the 0.54 meters SLR condition at the end of the century.

306 At Charchanga, the storm surge would be higher than the present day condition for TC Aila. For the mid-21st century under the
307 0.26 meters SLR scenario, storm surge would become 3.01 meters which is around 50% higher than the present day condition
308 (Figure 7d). And for the end of 21st century, this would become 68% higher than the present day as the SLR would reach 0.54 m
309 (Figure 7d).



310 The 0.26 m SLR for the mid-21st century would increase the water level, and the surge peak would be much higher at 2.4 m than
311 the present day observed value at 2.0 m (Figure 7a). Figure 7b shows the same comparison, but for a 0.54 m SLR in the end-of-
312 21st century scenario. For this case, the difference between the present day and end-of-21st century peak water level is much
313 higher than what we found in the mid-21st century climate scenario.

314

315 **4. Discussions**

316

317 In this paper, we showed that even if the future TCs remain the same strength like the present day ones their impact will be much
318 higher in a changing climate due to the effect of SLR. Several other factors not included in the modeling could make the storm
319 surge and inundation situation far worse than that shown in the modeling result. These factors include mangrove coverage
320 decrease, morphological changes, TC strength increase, and upstream river discharge changes.

321 For including the effect of future SLR in the model simulations, several methodologies were examined. One of the methods that
322 we experimented in this study was to include the increased sea level in open ocean boundary instead of adding it in to the whole
323 ocean depth by keeping the coastline fixed. In such case, an additional pressure gradient force was found acting towards the coast
324 which made the inundated area much higher.

325

326 In order to make the future SLR simulation realistic, we considered the increased sea level in ocean bathymetry and increased the
327 depth by 0.26 and 0.54 m, respectively, by considering land submergence near the coast. In that case, the result looked much
328 realistic than the previous one and this is the method we followed in this paper. For example, for the case of TC Aila under the
329 end-of-21st century scenario where we used a SLR of 0.54 m SLR at the open ocean boundary instead of adding it to ocean
330 depth and using the hydrodynamic conditions from the present day, the total inundated area was found to be 79% higher than the
331 present day one. Similar to that, for the mid-21st century scenario (a 0.26 m SLR), the inundated area was found to be 69% more
332 than the present day scenario. But when we added the SLR in ocean depth, the mid-21st century and end-of 21st century inundated
333 area was found to be 28% and 46% higher than the present day scenario. This increase in inundated area was much less than the
334 one that we found by adding the SLR in the open ocean boundary. Figure 8 displays the differences in inundated area based on
335 the consideration of SLR in the model input.

336 As discussed, TC Sidr made landfall near Sundarban, where the mangrove forest zone acted as a buffer in reducing the impact of
337 the storm surge flood. That is why, even though it was a TC 5, its impact was not as high as it might have been expected to be.
338 In this study, the roughness of the mangrove forest zone on the South-West part of Bangladesh was considered to be fixed for the
339 present day as well as for future scenarios. But Mukhopadhyay et al. (2015) predicted that 17% of the total mangrove cover
340 could disappear by 2105. If this decreasing trend of vegetation were considered in this study, the flooded area could be much
341 higher.

342 Morphological changes were not considered in this study. But according to Goodbred et al. (2003), each year the eastern estuary,
343 the central estuary and the western estuary are losing land at a rate of 0.13 cm/year, 0.16 cm/year and 0.16 cm/year, respectively.
344 This could also lead to increased inundated areas for future scenarios. But as the focus of the paper is to predict the future
345 scenario of storm surge and inundation due to the effect of SLR and comparisons with the present day scenarios, it is important
346 that we keep the roughness and morphological changes constant so that consistent comparisons can be made.



347 Some previous research showed that there could be increases in hurricane strength and landfall probability in the future due to
348 global climate change (Haarsma et al. 2013, Bender et al. 2010, Bengtsson et al. 2007). Though we slightly modified the present-
349 day TC strengths and selected 12 historical TC tracks to reduce landfall uncertainties and to make ensemble projection of future
350 storm surge inundation, strength may be much higher than the ones that we considered for this study. In such case, the
351 devastation could well be much higher under projected SLR conditions; which is very alarming

352 In this paper, we used the present-day river discharge data as an upstream boundary for generating future inundation scenarios.
353 But using the INCA-N, an Inland Catchment Modeling system and considering projected climatic & socio-economic scenarios,
354 Whitehead et al. (2015) showed that, there will be a significant increase in future monsoon intensities due to the impact of
355 climate change. That would make future flooding scenarios much worse than those experienced presently. So, based on the
356 changes in TC intensity, river discharges and land-use changes, the situation could well become more badly impacted than what
357 we found in this study.

358 The findings of our study are important for local governments to consider while they make new management and policy
359 decisions and to improve TC preparedness plans by increasing numbers of shelters and heights. Generally, in TC shelters, the
360 first floor is kept transparent due to the risk of high surge waters. Our study showed that, in the future, there will be an increase
361 in surge level from a minimum of 15% up to 70% if a TC 1 or a TC 5 makes landfall under increased SLR conditions. So, the
362 authority may consider increasing the height of the first floor considering the future risk of increase in storm surge level and
363 safety of local populations. Also, our model outputs showed that, the inundated area increase would range from 28%-53%
364 percent if there's any TC 1 or TC 5 were to make landfall with SLRs of 0.26 m or 0.54 m. This shows that a huge number of new
365 areas are going to face the impacts of storm surge inundation and by considering this issue, it is high time to increase the number
366 of TC shelters in the coastal areas of Bangladesh.

367 **5. Conclusion**

368

369 Employing the Delft3D-FLOW model, we simulated coastal storm surge and inundation for present day and future SLR
370 scenarios and compared the changes between them. After validating the present day model, simulations were conducted for mid-
371 21st century and end-of-21st century climate scenarios where the SLR has been considered as 0.26 m and 0.54 m respectively.
372 The model results showed that, with an increase of 0.26 m and 0.54 m SLR, there would be an increase of 38% and 48% of
373 inundated area respectively if TC Sidr was to make landfall with its present day strength. There would also be an increase of
374 25% and 34% in inundated area if category-1 TC Aila would make landfall with its present day strength but under the condition
375 of 0.26 m and 0.54 m respectively. Outputs from the ensemble projections showed that, even if the TC intensities, landfall
376 location and timings are uncertain, the probable range of inundated area would shift from 1000-1250 km² (present day) to 2000-
377 2250 km² (0.26 meter SLR) and 3500-3750 km² (0.54 meter SLR). Besides the inundated area, we also investigated the changes
378 in storm surge level if TC Sidr and TC Aila would make landfall under future SLR conditions. Similar to the inundated area,
379 increases in storm surge levels were found for future scenarios. The significant increase in simulated storm surge and inundation
380 hazards highlights the need for the local governments to improve cyclone preparedness in future SLR scenarios

381

382



383 **Acknowledgement**

384 The authors would like to thank Coastal Carolina University's Cyber-infrastructure project (<http://ci.coastal.edu>) for providing
385 access to computational resources. Also, we would like to acknowledge Dr. Susan Kay from Plymouth Marine Laboratory, UK
386 for her thoughtful opinions regarding the SLR input in model and Institute of Water and Flood Management, Bangladesh for
387 providing important data & support for this work.

388

389 **References:**

390 Ali, A.: Vulnerability of Bangladesh to climate change and sea level rise through tropical cyclones and storm surges, *Climate*
391 *Change Vulnerability and Adaptation in Asia and the Pacific*, Springer, pp. 171–179., doi: 10.1007/978-94-017-1053-4_16,
392 1996.

393 Alam, M.: Subsidence of the Ganges—Brahmaputra delta of Bangladesh and associated drainage, sedimentation and salinity
394 problems, *Sea-Level Rise and Coastal Subsidence*, Springer, pp. 169–192, doi:10.1007/978-94-015-8719-8_9, 1996.

395 Bender, M.A., Knutson, T.R., Tuleya, R.E., Sirutis, J.J., Vecchi, G.A., Garner, S.T., Held, I.M.: Modeled impact of
396 anthropogenic warming on the frequency of intense Atlantic hurricanes, *Science*, 327, 454–458, doi: 10.1126/science.1180568,
397 2010.

398 Bengtsson, L., Hodges, K.I., Esch, M., Keenlyside, N., Kornbluh, L., LUO, J.-J., Yamagata, T.: How may tropical cyclones
399 change in a warmer climate?, *Tellus a*, 59, 539–561, doi: 10.1111/j.1600-0870.2007.00251.x, 2007.

400 BODC.: Centenary Edition of the GEBCO Digital Atlas, published on CD-ROM on behalf of the Intergovernmental
401 Oceanographic Commission and the International Hydrographic Organization as part of the General Bathymetric Chart of the
402 Oceans. British oceanographic data centre, Liverpool, 2003.

403 Caesar, J., Janes, T., Lindsay, A.: Climate projections over Bangladesh and the upstream Ganges-Brahmaputra-Meghna system,
404 under review, *Environmental Science: Processes & Impacts (Under Review)*, 2017.

405 Egbert, G. D., Bennett, A. F. and Foreman, M. G. G.: TOPEX/POSEIDON tides estimated using a global inverse model, *J.*
406 *Geophys. Res.*, 99(C12), 24821–24852, doi:10.1029/94JC01894, 1994.

407 Goodbred, S.L., Kuehl, S.A., Steckler, M.S., Sarker, M.H.: Controls on facies distribution and stratigraphic preservation in the
408 Ganges–Brahmaputra delta sequence, *Sedimentary Geology*, 155, 301–316, doi:10.1016/S0037-0738(02)00184-7, 2003.

409 Haarsma, R.J., Hazeleger, W., Severijns, C., Vries, H., Sterl, A., Bintanja, R., Oldenborgh, G.J., Brink, H.W.: More hurricanes to
410 hit western Europe due to global warming, *Geophysical Research Letters*, 40, 1783–1788, doi: 10.1002/grl.50360, 2013.

411 Haque, C.E.: Atmospheric hazards preparedness in Bangladesh: a study of warning, adjustments and recovery from the April
412 1991 cyclone, *Earthquake and Atmospheric Hazards*, Springer, pp. 181–202, doi: 10.1007/978-94-011-5034-7_6, 1997.

413 Harris, D. L.: Characteristics of the hurricane storm surge, *Tech. Pap.*, 48, U. S. Weather Bur., Washington, D. C., 139 pp, 1963.

414 Hearn, C. J.: *The dynamics of coastal models*. Cambridge University Press, 2008.

415 Heming, J. T., Chan, J. C. L. and Radford, A. M.: A new scheme for the initialization of tropical cyclones in the UK
416 Meteorological Office global model, *Met. Apps*, 2, 171–184, doi:10.1002/met.5060020211, 1995.

417 Holland, G. J.: An analytic model of the wind and pressure profiles in hurricanes, *Monthly weather review*, 108(8), 1212-1218,
418 doi:10.1175/1520-0493(1980)108<1212:AAMOTW>2.0.CO;2, 1980.



- 419 Hydraulics, D.: Delft3D-FLOW user manual. Delft, the Netherlands, 2006.
- 420 Karim, M.F., Mimura, N.: Impacts of climate change and sea-level rise on cyclonic storm surge floods in Bangladesh, *Global*
421 *Environmental Change*, 18, 490–500, doi: 10.1016/j.gloenvcha.2008.05.002, 2008.
- 422 Knutson, T.R., McBride, J.L., Chan, J., Emanuel, K., Holland, G., Landsea, C., Held, I., Kossin, J.P., Srivastava, A.K., Sugi, M.:
423 Tropical cyclones and climate change, *Nature Geoscience*, 3, 157–163, doi: 10.1038/ngeo779, 2010.
- 424 Meehl, G.A., Covey, C., Delworth, T., Latif, M., McAvaney, B., Mitchell, J.F.B., Stouffer, R.J., Taylor, K.E., and Coauthors.:
425 Global climate projections. *Climate Change 2007: The Physical Science Basis*, S. Solomon et al., Eds. Cambridge University
426 Press, 2007.
- 427 Milliman, John D., James M. Broadus, and Frank Gable.: Environmental and economic implications of rising sea level and
428 subsiding deltas: the Nile and Bengal examples, *Ambio*, 18 (6), 340-345, doi: , 1989.
- 429 Mohal, N., Khan, Z.H., Rahman, N.: Impact of sea level rise on coastal rivers of Bangladesh. Dhaka: Institute of Water
430 Modelling (IWM). Assessment conducted for WARPO, an organization under Ministry of Water Resources, 2006.
- 431 Mukhopadhyay, A., Mondal, P., Barik, J., Chowdhury, S.M., Ghosh, T., Hazra, S.: Changes in mangrove species assemblages
432 and future prediction of the Bangladesh Sundarbans using Markov chain model and cellular automata, *Environmental Science:*
433 *Processes & Impacts*, 17, 1111–1117, doi: 10.1039/C4EM00611A, 2015
- 434 Murty, T.S., Flather, R.A., Henry, R.F.: The storm surge problem in the Bay of Bengal. *Progress in Oceanography*, 16, 195–233,
435 doi: 10.1016/0079-6611(86)90039-X ,1986.
- 436 Nash, J.E., Sutcliffe, J.V.:River flow forecasting through conceptual models part I—A discussion of principles, *Journal of*
437 *hydrology*, 10, 282–290, doi:10.1016/0022-1694(70)90255-6, 1970.
- 438 Pietrafesa, L. J., Janowitz, G. S., Chao, T. Y., Weisberg, R. H., Askari, F., & Noble, E.: The physical oceanography of Pamlico
439 Sound. University of North Carolina Sea Grant Publication UNC-WP-86-5, Raleigh, North Carolina, 125, 1986
- 440 Pietrafesa, L.J., Bao, S., Yan, T., Slaterry, M., Gayes, P.T.: On Sea Level Variability and Trends in United States Coastal Waters
441 and Relationships with Climate Factors, *Advances in Adaptive Data Analysis*, 7, 1550005, doi: 10.1142/S1793536915500053,
442 2015.
- 443 Sakib, M., Nihal, F., Haque, A., Rahman, M., Ali, M.: Sundarban as a Buffer against Storm Surge Flooding, *World Journal of*
444 *Engineering and Technology*, 3, 59, doi: 10.4236/wjet.2015.33C009, 2015.
- 445 SMRC.: The Vulnerability Assessment of the SAARC Coastal Region due to Sea Level Rise: Bangladesh Case, SAARC
446 Meteorological Research Center, Dhaka SMRC-No. 3, 2003.
- 447 Vatvani, D.K., Gerritsen, H., Stelling, G. S., Rao, A. K.: Cyclone induced storm surge and flood forecasting system for India.
448 *Solutions to Coastal Disasters '02*, San Diego, CA, 2002.
- 449 Warrick, R.A., Bhuiya, A.A.H., Mitchell, W.M., Murty, T.S., Rasheed, K.B.S.: Sea-level Changes in the Bay of Bengal, in: *The*
450 *Implications of Climate and Sea-Level Change for Bangladesh*, Springer, pp. 97–142, 1996.
- 451 Whitehead, P.G., Barbour, E., Futter, M.N., Sarkar, S., Rodda, H., Caesar, J., Butterfield, D., Jin, L., Sinha, R., Nicholls, R.,
452 others.: Impacts of climate change and socio-economic scenarios on flow and water quality of the Ganges, Brahmaputra and
453 Meghna (GBM) river systems: low flow and flood statistics, *Environmental Science: Processes & Impacts*, 17, 1057–1069, doi:
454 10.1039/C4EM00619D, 2015.
- 455 Xie, L., Bao, S., Pietrafesa, L.J., Foley, K., Fuentes, M.: A real-time hurricane surface wind forecasting model: Formulation and
456 verification, *Monthly Weather Review*, 134, 1355–1370, doi:10.1175/MWR3126.1, 2006.



457 Zhang, K., Liu, H., Li, Y., Xu, H., Shen, J., Rhome, J., Smith, T.J.: The role of mangroves in attenuating storm surges, *Estuarine,*
458 *Coastal and Shelf Science* 102, 11–23, doi: 10.1016/j.ecss.2012.02.021, 2012.

459

460

461

462

463

464

465

466

467

468

469

470

471

472

473

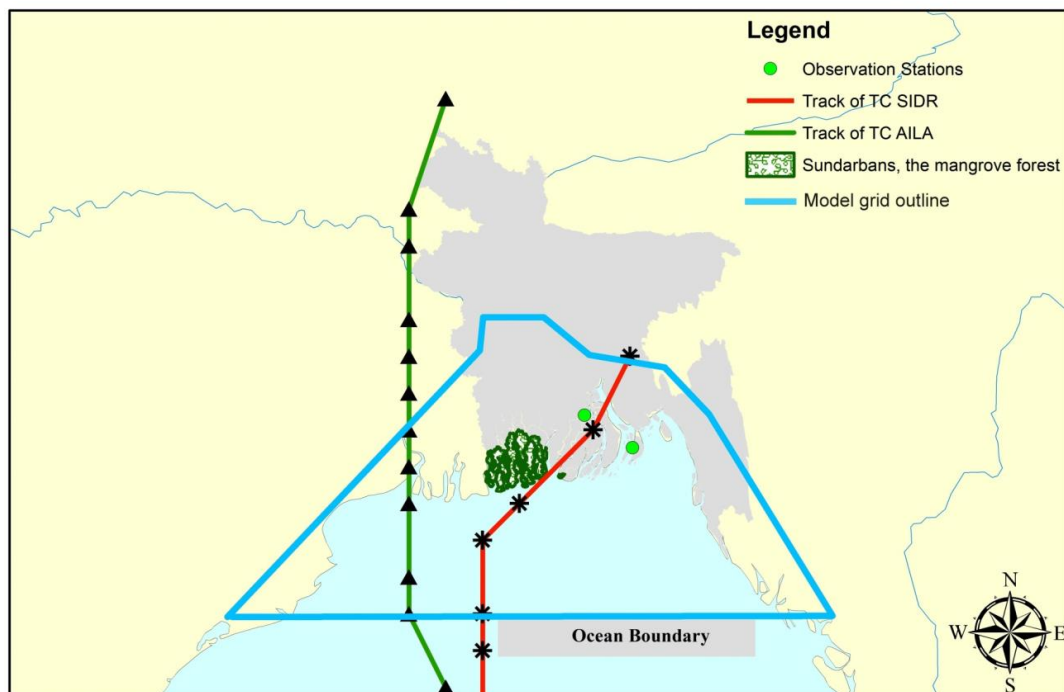
474

475

476

477

478



479

480 **Figure 1.** Map showing the study area for this work. The red and green lines representing the tracks of TC Sidr and TC Aila respectively. Area
481 marked with green color indicates the Sundarban mangrove forest region. Two green circles over the study area are the observation stations of
482 Bangladesh Inland Water Transport Authority (BIWTA). The blue colored outline shows the extent of model grid over the region.

483

484

485

486

487

488

489

490

491

492



493

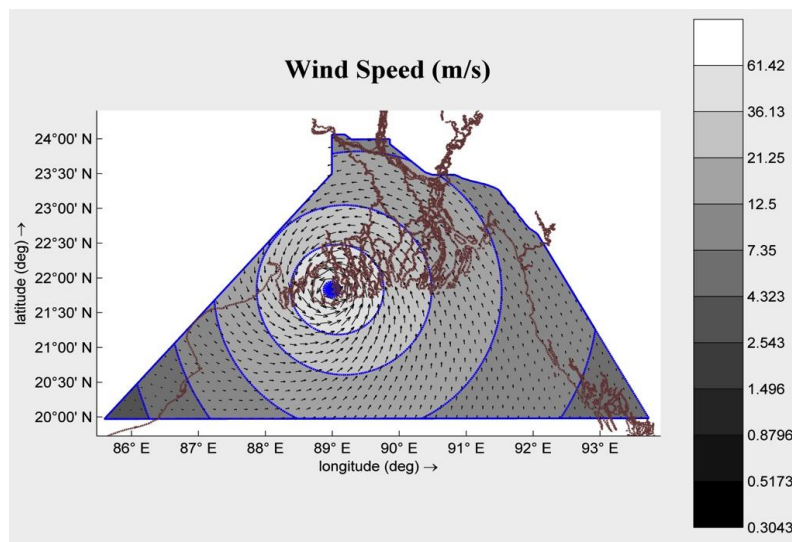


Figure 2. Distribution of wind field over the model domain for TC Sidr during landfall generated using Holland's Equation.

494

495

496

497

498

499

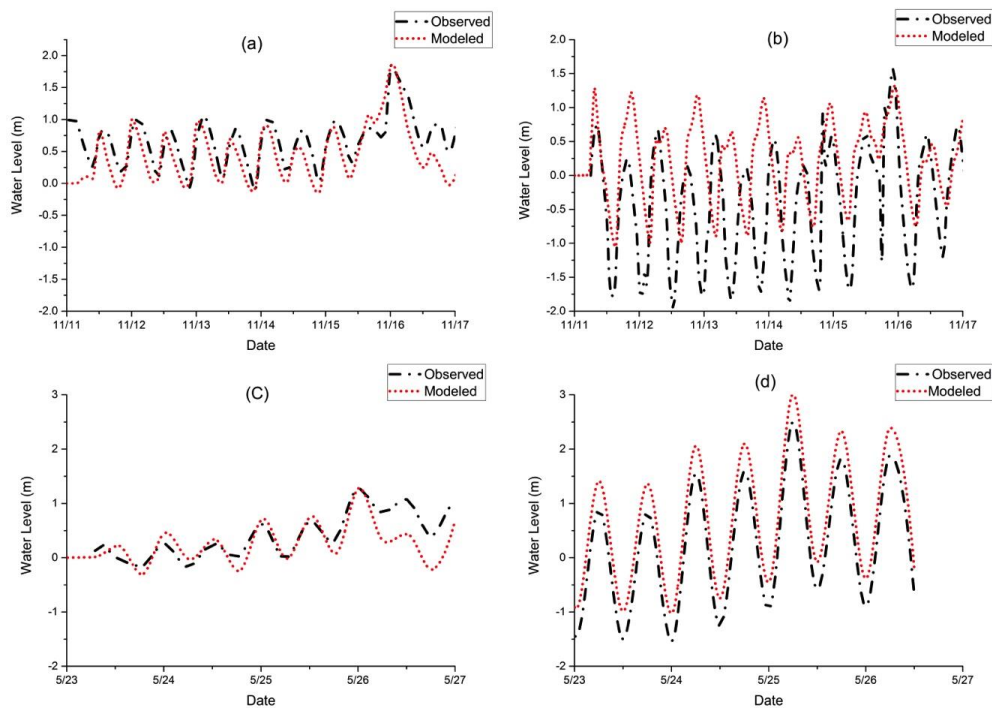
500

501

502

503

504

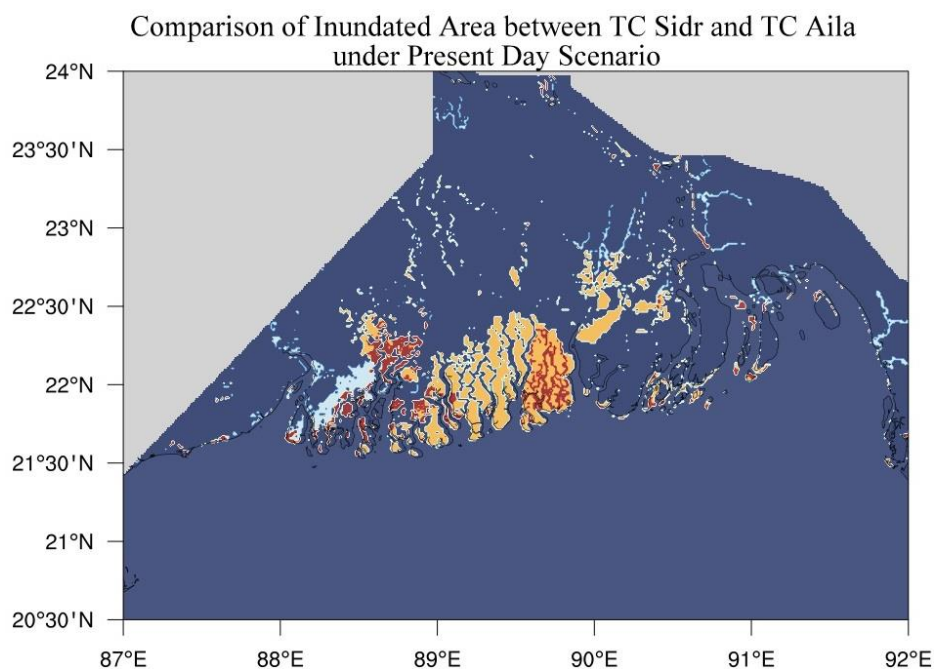


505
506 **Figure 3.** Comparison of observed and modeled Water Level for TC Sidr and TC Aila in Barisal and Charchanga observation stations. (a)
507 Measured and Modeled Water Level comparison for TC Sidr in Barisal, (b) Measured and Modeled Water Level comparison for TC Sidr in
508 Charchanga, (c) Measured and Modeled Water Level comparison for TC Aila in Barisal, (d) Measured and Modeled Water Level comparison
509 for TC Aila in Charchanga.

510
511
512
513
514
515
516



517



518

Figure 4. Yellow colors denotes the areas flooded by TC Sidr but not in Aila, and the white color representing the area inundated by TC Aila but not in Sidr. Red color is the area flooded by both TC Sidr and TC Aila. Blue color is showing the non-flooded area (either land or constant water).

519

520

521

522

523

524

525



526

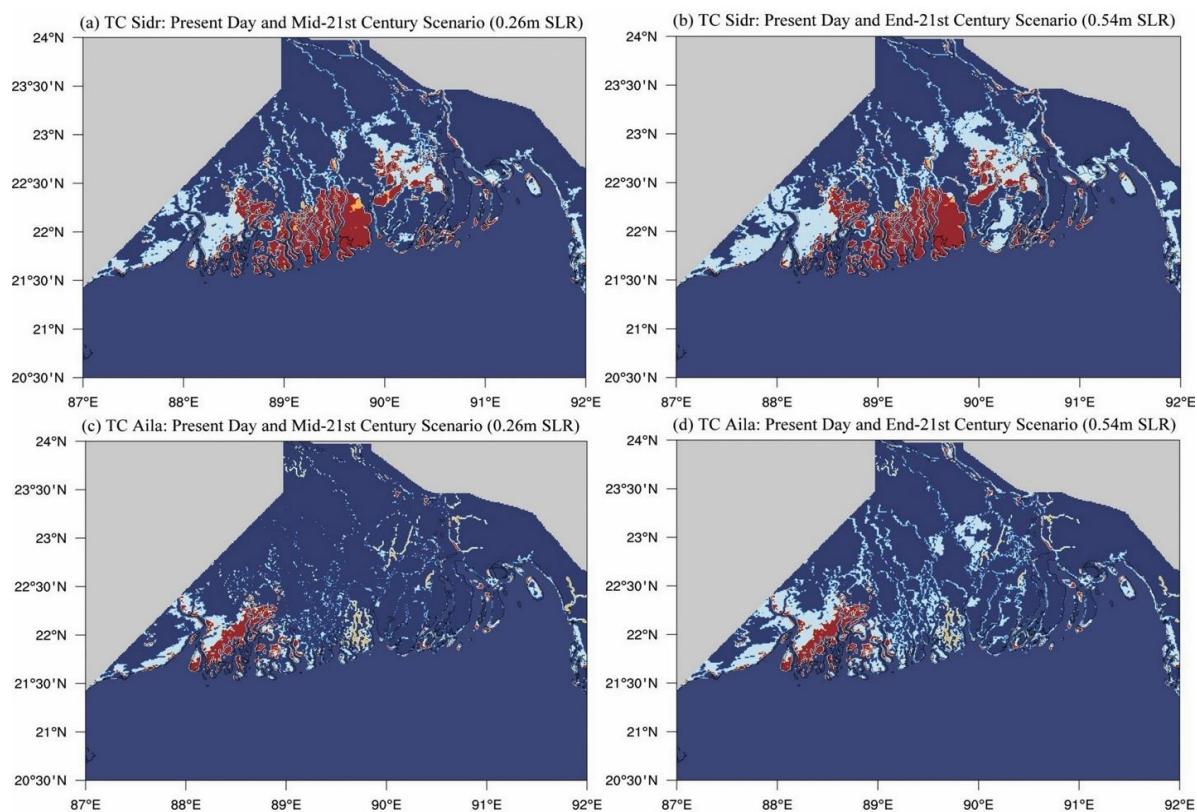


Figure 5: Comparison of inundated area between present day and future climate scenarios for (a) TC Sidr mid-21st century 0.26m SLR (b) TC Sidr end-21st century 0.54m SLR (c) TC Aila mid-21st century 0.26m SLR (d) TC Aila end-21st century 0.54m SLR. White color is representing the increased flooded areas that were not in present day scenario but the increase due to future SLR. Red color is showing the inundated areas that were similar both for present day and future SLR scenario case. Blue areas are non-flooded areas. Yellow color is showing the areas that were part of present day inundation but was not flooded during the future SLR conditions.

527

528

529

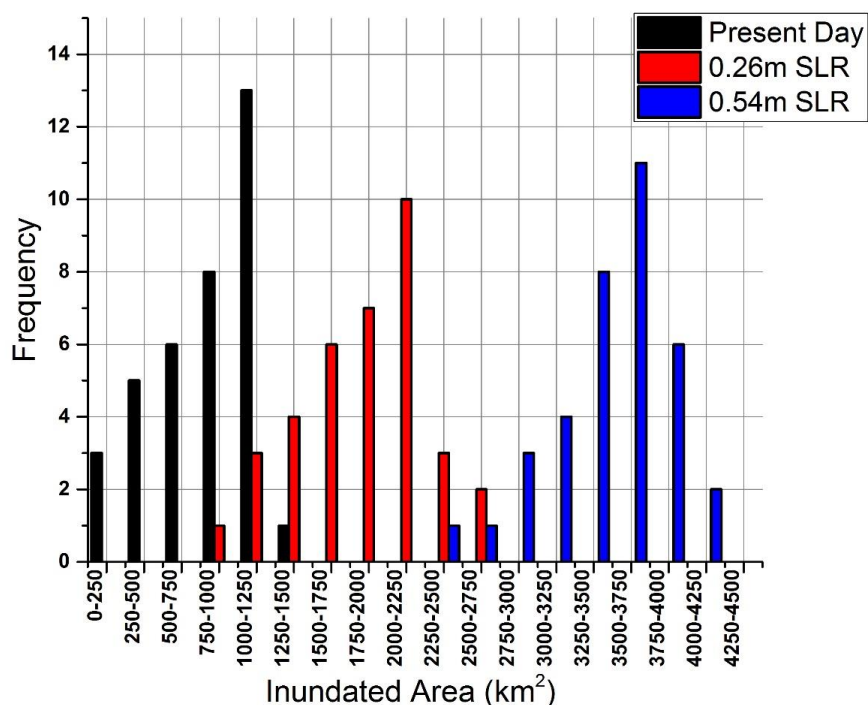
530

531

532

533

534



535

536 **Figure 6:** Ensemble projection of the future SLR impact on storm surge inundation. The column in black color is representing the inundation
537 events for present day sea level condition, red colored one is for 0.26 meter of SLR and blue colored column is for 0.54 meter of SLR
538 conditions. In total 108 simulations were conducted for present and two future SLR scenarios.

539

540

541

542

543

544

545



546

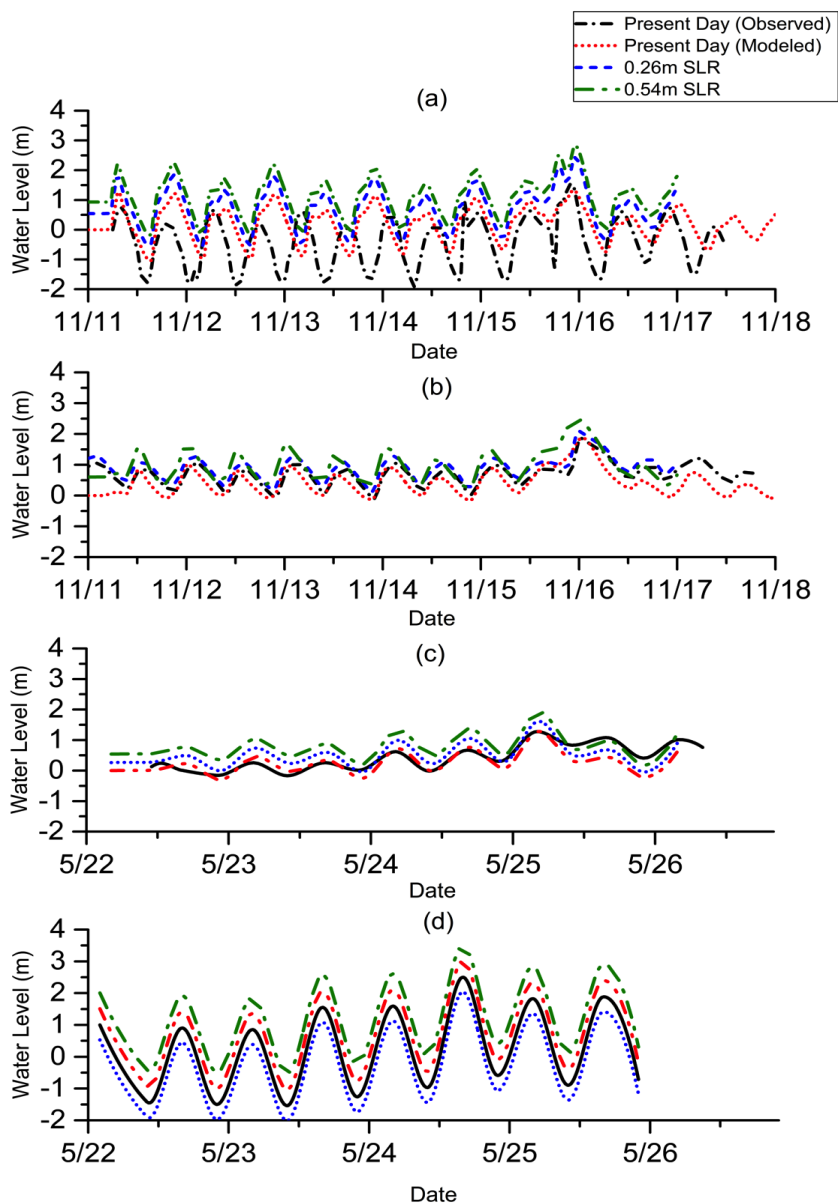
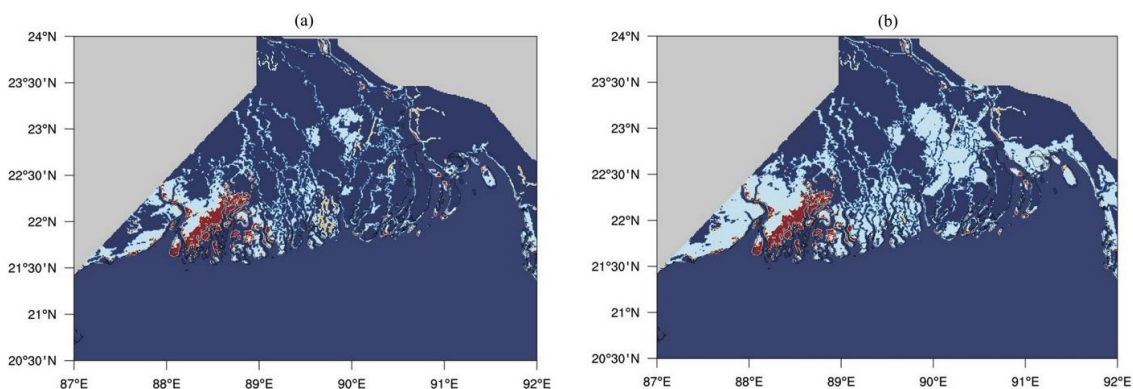


Figure 7. Comparison of water level for TC Sidr and TC Aila at Barisal and Charchanga Station between present day and future climate scenarios. (a) Comparison between present day and mid-21st century scenario (0.26m SLR) for TC Sidr in Barisal Station, (b) Comparison between present day and end-21st century scenario (0.54m SLR) for TC Sidr in Charchanga station, (c) Comparison between present day and mid-21st century scenario (0.26m SLR) for TC Aila in Barisal Station, (d) Comparison between present day and end-21st century scenario (0.54m SLR) for TC Aila in Charchanga station.



547
548
549
550



551

552 **Figure 8.** Comparison of inundated areas for TC Aila between present day and end-21st century (0.54m SLR) scenario. White color is
553 representing the increased flooded areas that were not in present day scenario but the increase due to future SLR. Red color is showing the
554 inundated area that's similar both for present day and future scenario case. Blue areas are either land or constant waters (those which are
555 already water at the model initialization time). Figure (a) is representing the inundated area when SLR was considered on ocean depths instead
556 of adding it in to the open ocean boundary and figure (b) showing the inundated area when we considered the SLR on ocean boundary.

557
558
559
560
561
562
563
564
565
566
567
568
569
570
571
572



573

574

575

Table 1 Manning's Roughness Coefficient for different land coverings.

| Land cover | Manning's coefficient |
|------------|-----------------------|
| River | 0.015 |
| Mangrove | 0.080 |
| Ocean | 0.01 |
| Land | 0.025 |

576

577

578

579 **Table 2:** Parameters considered for ensemble projection of storm surge inundation which includes the TC intensities, tidal conditions and the
 580 SLR scenarios.

| TC name | Intensities | Tide conditions | SLR |
|-------------------------|----------------------------|--|--|
| TC Sidr | +10%, present day, -10% | High Tide, low tide, actual tide, zero tide | Present day, 0.26 meter, 0.54 meter |
| TC Aila | +10%, Present day, -10% | High Tide, low tide, actual tide, zero tide | Present day, 0.26 meter, 0.54 meter |
| 12 historical TC tracks | Actual intensities | Actual tide conditions | Present day, 0.26 meter, 0.54 meter |

581

582

583 **Table 3.** Computed values of RMSE, MAE and Nash-Sutcliffe coefficient for both TC Sidr and TC Aila

| Stations | TC Sidr | | | TC Aila | | |
|----------------|--------------|--------------|--------------|--------------|--------------|-------------|
| | RMSE (m) | MAE (m) | NASH | RMSE (m) | MAE (m) | NASH |
| Barisal | 0.23 | 0.16 | 0.85 | 0.33 | 0.24 | 0.65 |
| Charchanga | 0.26 | 0.19 | 0.80 | 0.28 | 0.17 | 0.73 |
| Average | 0.245 | 0.175 | 0.825 | 0.305 | 0.205 | 0.69 |